HHS Public Access

Author manuscript

Alcohol Clin Exp Res. Author manuscript; available in PMC 2023 December 01.

Published in final edited form as:

Alcohol Clin Exp Res. 2022 December ; 46(12): 2163–2176. doi:10.1111/acer.14954.

Hepatic CYP2B10 is highly induced by binge ethanol and contributes to acute-on-chronic alcohol-induced liver injury

Bryan Mackowiak[1,*], **Mingjiang Xu**[1,*], **Yuhong Lin**[1], **Yukun Guan**[1], **Wonhyo Seo**[1], **Ruixue Ren**[1], **Dechun Feng**[1], **Jace W. Jones**[2], **Hongbing Wang**[2], **Bin Gao**[1]

[1]Laboratory of Liver Diseases, National Institute on Alcohol Abuse and Alcoholism, National Institutes of Health, Bethesda, MD 20892, USA;

[2]Department of Pharmaceutical Sciences, University of Maryland School of Pharmacy, 20 Penn Street, Baltimore, MD 21201, USA

Abstract

Background: The chronic-plus-binge model of ethanol consumption, where chronically (8-week) ethanol-fed mice are gavaged a single dose of ethanol (E8G1), is known to induce steatohepatitis in mice. However, how chronically ethanol-fed mice respond to multiple binges of ethanol remains unknown.

Methods: We extended the E8G1 model to 3 gavages of ethanol (E8G3) spaced 24h apart, sacrificed each group 9h after the final gavage, analyzed liver injury, and examined gene expression changes using microarray analyses in each group to identify mechanisms contributing to liver responses to binge ethanol.

Results: Surprisingly, E8G3 treatment induced lower levels of liver injury, steatosis, inflammation, and fibrosis as compared to mice after E8G1 treatment. Microarray analyses identified several pathways that may contribute to the reduced liver injury after E8G3 treatment compared to E8G1 treatment. Cytochrome P450 2B10 (*Cyp2b10*) was one of the top upregulated genes in the E8G1 group and further upregulated in the E8G3 group, but only moderately induced after chronic ethanol consumption, which was confirmed by RT-qPCR and western blot analyses. Genetic disruption of the *Cyp2b10* gene worsened liver injury in E8G1 and E8G3 mice with higher blood ethanol levels compared to wild-type control mice, while *in vitro* experimentation revealed that CYP2b10 did not directly promote ethanol metabolism. Metabolomic analyses revealed significant differences in hepatic metabolites from E8G1-treated *Cyp2b10* knockout and WT mice, and these metabolic alterations may contribute to the reduced liver injury in *Cyp2b10* knockout mice.

Conclusion: Hepatic *Cyp2b10* expression is highly induced after ethanol binge, and such upregulation reduces acute-on-chronic ethanol-induced liver injury via the indirect modification of ethanol metabolism.

Corresponding author: Bin Gao, M.D., Ph.D., Laboratory of Liver Diseases, NIAAA/NIH, 5625 Fishers Lane, Bethesda, MD 20892, USA; Tel.: 301-443-3998; bgao@mail.nih.gov.

*Bryan Mackowiak and Mingjiang Xu contributed equally to this work

Conflicts of interest: All authors disclose no conflicts.

Introduction:

Alcohol use is a major cause of mortality worldwide, with alcohol-associated liver disease (ALD) being one of the most detrimental aspects of alcohol abuse (Griswold et al., 2018). Chronic abuse of alcohol is known to promote the development of fatty liver, but how and when chronic drinkers progress to more harmful phenotypes are poorly understood (Gao and Bataller, 2011). Severe alcoholic hepatitis (AH) is one of the most damaging types of ALD that exhibits a high short-term mortality rate, and its onset is associated with recent excessive alcohol consumption (Lucey et al., 2009). While the compensatory mechanisms behind liver adaptation to chronic alcohol intake have been studied, how the liver responds to bouts of excessive drinking, alone or in addition to chronic drinking, is relatively unknown. Since the pattern of alcohol intake is known to be related to the risk of alcohol-induced liver damage, understanding how the liver develops compensatory mechanisms against binge drinking-induced injury is increasingly important (Bellentani et al., 1997).

After typical levels of alcohol consumption, ethanol is eliminated via oxidation in the liver to acetaldehyde, which is further metabolized to acetate. The major ethanol oxidation pathway in the liver involves alcohol dehydrogenase 1 (ADH1), which has a low Km for ethanol making it the preferential enzyme for clearance of low levels of ethanol. In addition, the cytochrome P450-dependent microsomal ethanol oxidizing system (MEOS), which plays a minor role in basal liver ethanol metabolism, is highly induced after chronic alcohol consumption or high blood ethanol concentrations (Zakhari and Li, 2007). The most prominent member of this system is the chronic ethanol-inducible enzyme CYP2E1, which participates in the clearance of ethanol but also contributes to long-term alcohol-induced liver injury, mainly due to its generation of reactive oxygen species (ROS) (Gonzalez et al., 1991, Cederbaum, 2010). The CYP2B family of enzymes is also known to be slightly induced upon chronic and binge ethanol administration, but its role in alcohol-induced liver injury and ethanol metabolism is unknown (Koga et al., 2016, Schoedel et al., 2001).

Studying the pathogenesis of ALD in preclinical models is challenging due to much higher rates of ethanol metabolism in rodents when compared with humans (Cederbaum, 2012). Several models used to study acute ethanol-induced organ injury involve giving rodents 3 consecutive binges (typically every 12h) and sacrificing 3–9h after the final binge. This approach has been used to successfully identify key molecular determinants of acute ethanol-induced heart, pancreas, adipose, and liver injury (Ghosh Dastidar et al., 2018). Another model that successfully recapitulates some features of AH has been widely used to study ALD progression and potential treatments in mice is the NIAAA model of chronic-plus-binge ethanol, where mice are given chronic ethanol for 10 days to 8 weeks and given a single binge to provoke ethanol-induced organ injury (Xu et al., 2015, Bertola et al., 2013a). However, liver injury in the NIAAA model is significantly decreased within 24h of the binge, making it difficult to study factors that may contribute to repeated instances of liver injury. In the current study, we sought to combine the 8-week chronic-plus-binge model with the 3 consecutive binge model to better understand how multiple binges in a row on top of chronic ethanol consumption can affect liver injury and identify detrimental or protective mechanisms.

Materials and Methods:

Mice.

C57BL/6N mice were purchased from the National Cancer Institute (NCI, Frederick, MD, USA). C*yp2b10* knockout (KO) mice were generated in the UC Davis Knockout Mouse Project (KOMP) Repository (Strain ID: *Cyp2b10*$^{tm1a(KOMP)Wtsi}$) and were backcrossed to a C57BL/6N background for more than 10 generations. C*yp2b10* KO mice were genotyped using long range polymerase chain reaction (PCR) according to the KOMP-CSD standard protocol. The 5' genotyping primers were: 5' Universal (LAR3) – CACAACGGGTTCTTCTGTTAGTCC; and 5' Gene Specific (GF4) – CAACATGGAGAACTGGCCATTAGC for a 5119 base pair product. The 3' genotyping primers were: 3' Universal (RAF5) – CACACCTCCCCCTGAACCTGAAAC; and 3' Gene Specific (GR3) – CAACCAACACGTTAGTTCATTAGTCAATTC for an 8881 base pair product. After confirmation of the genotype, the C*yp2b10* KO mice were homozygous bred. *Adh1* KO mice were kindly provided by Dr. Duester (Burnham Institute, La Jolla, CA) (Deltour et al., 1999), and backcrossed to a C57BL/6N background for more than 10 generations. *Adh1* KO mice were genotyped as described previously (Anvret et al., 2012). All mouse experiments described in the current paper were reviewed and approved by the National Institute on Alcohol Abuse and Alcoholism Animal Care and Use Committee.

Ethanol Feeding Protocols.—Eight to twelve-week-old male or female mice were subjected to several different ethanol feeding protocols as described previously (Bertola et al., 2013b, Xu et al., 2015). **(1) Pair-fed for 8 weeks (P8w):** The mice were pair-fed an isocaloric control diet for 8 weeks, followed by gavage administration of isocaloric dextrin-maltose. **(2) Chronic feeding for 8 weeks (E8w):** The mice were initially fed a controlled Lieber-DeCarli diet *ad libitum* for 5 days (F1259SP, Bio-Serv, Flemington, NJ) to acclimatize them to a liquid diet. Subsequently, the ethanol-fed groups were allowed free access for 8 weeks to an ethanol diet (F1258SP, Bio-Serv) containing 5% (vol/vol) ethanol. **(3) Chronic (8 weeks)-plus-gavage feeding (E8G1):** The mice were fed as described for chronic feeding and mice received a single dose of ethanol (5 g/kg body weight) via gavage in the early morning and were sacrificed 9 hours later. **(4) Chronic (8 weeks)-plus-three gavages (E8G3):** Mice were fed an ethanol diet for 8 weeks as described above and gavaged once per 24 h (5g/kg ethanol) for 3 days. Mice were euthanized 9 hours post the third gavage. **(5) Acute gavage**: The mice received a single dose of ethanol (5 g/kg body weight) via gavage in the early morning and were sacrificed 3, 6, 9, 24, or 72 hours later. Mice were deeply anesthetized before blood collection from the orbital sinus into EDTA-coated tubes (Sardset) on ice or microcentrifuge tubes at room temperature for serum collection and euthanized via cervical dislocation. The liver, stomach, and intestines were harvested, quickly weighed (if applicable), and either snap frozen in liquid nitrogen or put in 10% formalin before further analysis.

Biochemical Assays.

Serum alanine aminotransferase (ALT) and aspartate aminotransferase (AST) levels were analyzed by a Catalyst Dx Chemistry Analyzer (IDEXX Laboratories, Inc., Westbrook, ME). Serum triglyceride and cholesterol levels were measured using colorimetric/

fluorometric assay kit (Cayman Chemical Company, Ann Arbor, MI), according to the assay protocol. Hydroxyproline was measured using a commercial kit from BioVision (Milpitas, CA) following the manufacturer's instructions.

Histology and Immunohistochemistry.

Tissue specimens were fixed in 10% buffered formalin and embedded in paraffin. Then, 4-μm sections were used for staining (hematoxylin and eosin (H&E) or Sirius red dyes (MilliporeSigma)) and immunohistochemistry. Immunohistochemical staining for myeloperoxidase (MPO), α-smooth muscle actin (α-SMA), and CYP2B10 was performed using a prediluted rabbit anti-MPO polyclonal antibody (Biocare Medical, LLC, Concord, CA), a monoclonal mouse anti-α-SMA (A2547; Sigma, St. Louis, MO), and a rabbit anti-CYP2B10 antibody (EMD Millipore, Billerica, MA), respectively. Then, Vectastain rabbit/mouse avidin/biotin complex (ABC) staining kit (Vector Laboratories, Inc., Burlingame, CA), was used according to the manufacturers' instructions for visualization.

Microarray Analyses of Mouse Liver Samples.

Liver samples from P8w, E8w, E8G1, and E8G3 were subjected to microarray analysis at the same time. Dye-coupled cDNAs were purified with a MiniElute PCR purification kit (Qiagen) and hybridized to an Agilent 44K mouse 60-mer oligo microarray (Agilent Technologies, Santa Clara, CA). The data were processed and normalized using the Genespring GX software package (Agilent Technologies). The P8w, E8w, E8G1 microarray data were previously published and deposited in NCBI's Gene Expression Omnibus (No. GSE67546)(Xu et al., 2015). The E8G3 microarray data are deposed in NCBI's Gene Expression Omnibus (GSE212755). Differential expression analysis was performed via the R package DESeq2 (v1.30.1). Genes with fold change >1.5 and padj <0.05 were put into gene set enrichment analysis via the R package clusterProfiler (v3.18.1). The R package pheatmap (v1.0.12) was used to create the heatmap plots. Interactive Venn diagrams and gene function analyses were processed by Ingenuity Pathway Analysis (IPA). The human ALD RNA-Seq data were obtained from Kim et al. (Kim et al., 2021) analyses of Argemi et al. (Argemi et al., 2019).

Real-time Quantitative Polymerase Chain Reaction (RT-qPCR).

Total cellular RNA was isolated from the liver using a RNeasy mini kit (QIAGEN Inc., Valencia, CA). One microgram of total RNA was reverse-transcribed by random priming and incubation with 200 U of Moloney murine leukemia virus transcriptase at 37°C for 1 hour. The resulting single-stranded cDNA was then subjected to real-time PCR analyses with 18 S as internal controls. The primer sequences used are shown in Supporting Table 1.

Microsome Isolation.

Microsomes were prepared as described previously (Sahi et al., 2000) with some modifications. Mouse liver tissue samples were snap frozen on dry ice and stored at −80°C until processing with all further procedures completed at 4°C. Ice-cold homogenization buffer (50 mM Tris-HCl, pH 7.0, 150 mM KCl, 2 mM EDTA) was added to tissue and processed with a handheld tissue homogenizer before a 15 second sonication. Homogenates

were spun at 9,000 *g* for 20 min. The supernatant was transferred to ultracentrifuge tubes and spun at 100,000 *g* for 45 min. The supernatants were removed, and the microsomal pellet was resuspended in 0.25 M sucrose. Protein concentrations of the subcellular fractions were determined using the Pierce bicinchoninic acid (BCA) protein assay kit (ThermoFisher Scientific Inc., Grand Island, NY).

Enzyme Assays.

To determine CYP2b activity, 10 μM pentoxyresorufin (Tocris), a selective CYP2b substrate (Lubet et al., 1985), was incubated with control or induced (TCPOBOP) microsomes with or without the selective CYP2b inhibitor 2-Phenyl-2-(1-piperidinyl) propane preincubation (PPP, Cayman Chemicals) (Chun et al., 2000). Microsomes were preincubated at 10x concentration (0.5 mg/mL) with PPP (30 μM) in incubation buffer (100 mM phosphate buffer (pH 7.4), 2 mM $MgCl_2$, 5 mM glucose-6-phosphate, 1 mM NADP, 0.5 U/mL glucose-6-phosphate dehydrogenase) for 30 min to inactivate CYP2b (Walsky and Obach, 2007). Microsomes from preincubations (10 μL) were spiked into substrate-containing incubation buffer with a final volume of 0.1 mL and a final microsomal concentration of 0.05 mg/mL. Ethanol concentrations for microsome incubations ranged from 5 – 200 mM. Acetaldehyde levels were measured by using gas chromatography mass spectrometry as described previously (Ren et al., 2020).

Western Blot Analyses.

Western blotting was performed as described previously (Ki et al., 2010). Protein bands were visualized by SuperSignal™ West Femto Maximum Sensitivity Substrate (Thermo Fisher Scientific Inc, Grand Island, NY). Antibodies for ADH1 and β-actin were purchased from Cell Signaling Technology (Danvers, MA); anti CYP2B10 and CYP2E1 were purchased from Millipore (Billerica, MA). GAPDH was purchased from Abcam (Waltham, MA).

Untargeted Metabolomics.

Materials. LC-MS grade acetonitrile, methanol, water, and formic acid were purchased from Fisher Scientific (Pittsburg, PA). All chemicals and reagents were used without further purification. *Metabolite extraction*. Metabolites were extracted from plasma and liver tissues as follows. For plasma samples, 25 μL of plasma was combined with 500 μL of cold acetonitrile. For the tissue samples, 10 mg of tissue was homogenized in 200 μL of cold methanol with 5 mM PBS. An additional 400 μL of cold acetonitrile was added to the tissue homogenate. The mixtures were thoroughly vortex mixed for 1 minute and stored at −80 °C for four hours. The samples were then centrifuged at 10,000 rpm for 10 min at 4 °C. Five hundred μL of supernatant was transferred and dried under a steady stream of nitrogen at 30 °C. The dried sample was resuspended in water/acetonitrile (1:1, v/v) with 0.1 % formic acid and stored at −20 °C until analysis. The protein pellet following the centrifugation step was used to determine the protein content via a BCA kit (bicinchoninic acid assay, Thermo Fisher Scientific, Rockford, USA). *Metabolite analysis*. The metabolite extracts were analyzed by liquid chromatography high-resolution mass spectrometry (LC HRMS). The LC HRMS analyses were performed on an Agilent 1290 Infinity LC coupled to an Agilent 6560 Quadrupole Time-of-Flight (Q-TOF) mass spectrometer (Agilent Inc.,

Santa Clara, CA, USA). The separation was achieved using a Waters BEH Amide (1.7 μm; 2.1 × 150 mm) column (Waters Corp., Milford, MA, USA). Mobile phase A was acetonitrile with 0.1% formic acid and mobile phase B was water with 0.1% formic acid. The gradient was held at 1% B for 0.1 min, ramped to 70% B in 6.9 min, ramped to 1% B in 0.1 min, and held at 1% B for 2.9 min. The flow rate was 0.4 mL/min. The column was maintained at 45 °C and the auto-sampler was kept at 5 °C. A 2 μL injection was used for both positive and negative ion mode. The MS parameters were as follows: extended dynamic range, 2 GHz; gas temperature, 300°C; gas flow, 10 L/min; nebulizer, 50 psi; sheath gas temperature, 350°C; sheath gas flow, 12 L/min; VCap, 3.5kV (+), 3.0kV (–); nozzle voltage, 250V; reference mass *m/z* 121.0509, m/z 1221.9906 (+), *m/z* 119.0363, *m/z* 980.0164 (–); range *m/z* 100–1000; acquisition rate, 3 spectra/s. Data were acquired with MassHunter version B.09.00 (Agilent Inc.,). LC HRMS data was analyzed with Profinder v10.0 (Agilent Inc.) and MetaboAnalyst 5.0 (Pang et al., 2021). Raw data files were directly imported into Profinder where retention time alignment, peak picking, deconvolution of adducts, peak integration, and determination of abundance were performed. Preliminary identification involved accurate mass correlation at a threshold of 10 ppm to the human metabolome database (HMDB) (Wishart et al., 2022). The processed data generated from Profinder which included peak area and *m/z* value was exported into MetaboAnalyst for statistical analyses. Raw data has been uploaded to Mendeley Data (LCMS dataset_Hepatic CYP2B10 is highly induced by binge ethanol; DOI:10.17632/y2jxf74jyv.1).

Statistical analysis—Data are presented as the mean ± SEM. Statistical analysis was performed with GraphPad Prism software (v. 9.0; GraphPad Software, La Jolla, CA). Significance of data with multiple groups was evaluated via two-sided one-way or two-way ANOVA with Tukey's post hoc test dependent upon whether there were two types of variables (i.e. treatment group and mouse genotype) or a single variable (i.e. different treatment groups). Comparisons were considered statistically significant at P values of < 0.05.

Results:

Liver adapts to bouts of binge drinking with less injury and fewer gene alternations after three binges than one binge in chronically ethanol-fed mice

We have previously demonstrated that one binge markedly exacerbates liver damage and fibrogenic response in chronically ethanol-fed mice (Bertola et al., 2013b, Xu et al., 2015). To examine whether three consecutive binges cause more liver damage than one binge, we subjected chronically ethanol-fed mice to either a single binge or a binge every 24h for 3 days. Surprisingly, ethanol-fed mice given three binges (E8G3) exhibited less liver damage than ethanol-fed mice given one binge (E8G1). Serum ALT and AST, and hepatic TG levels were much lower in the E8G3 group than those in E8G1 group (Fig. 1A). Liver-to-body weight ratio was only increased after E8G1 but not E8G3 (Fig. S1A–B). Liver histology and immunohistochemistry analyses revealed that E8G3 had less steatosis and liver fibrosis (as shown by α-SMA and Sirius Red staining) than E8G1 (Fig. 1B). Hepatic levels of hydroxyproline, a marker for liver fibrosis, was elevated in E8G1 but not in E8G3 mice (Fig. 1C). Quantitative RT-PCR analyses demonstrated that hepatic expression of the

steatosis-associated gene *Fsp27a/b* and several fibrosis-associated genes (*Col1a1*, *Col4a2*, *Col5a2*, *Col12a1*) was highly upregulated in E8G1 but not in E8G3 mice compared to those in E8w or P8w group (Fig. 1D; Fig. S1C).

One binge activates multiple hepatoprotective pathways that may contribute to the adaption to the subsequent binges in chronically ethanol-fed mice.

To determine how the liver responds to bouts of binge drinking, we performed microarray analyses on liver tissue from mice in the P8w, E8w, E8G1, and E8G3 groups. Principal component analysis (PCA) (Fig. 2A) showed that while the P8w and E8w groups generally cluster together, the E8G1 group separated via principal component (PC) 1 and 2, while E8G3 only separated from P8w and E8w by PC1. The heatmap of gene alternations between E8w and E8G1 revealed that E8G1 caused alterations of many genes in the liver compared to the P8w or E8w, but most of these changes in the E8G3 group were diminished and returned towards the levels of P8w or E8w (Fig. 2B). Looking at differences at the gene level, the volcano plot identified several genes known to be protective in ethanol-induced liver injury that are downregulated in E8G3 compared with E8G1, including *Lpin1* and *Gstm1*, while ethanol-injury promoting *Fabp4* and *Cidec* are also downregulated (Fig. 2C) (Attal et al., 2021, Hu et al., 2013, Xu et al., 2015, Roy et al., 2016). The most up- and downregulated genes in E8G3 vs. E8G1 are shown in Supporting Table 2.

To better understand the systemic changes in liver function between E8G1 and E8G3, we performed pathway analyses in Ingenuity Pathway Analysis (IPA) and KEGG comparing E8G1 and E8G3. In both analyses, oxidative phosphorylation, acute phase response/ complement/coagulation cascades, and glutathione metabolism were altered between E8G1 and E8G3 (Fig. 2D; Fig. S2A–B). The IPA upstream regulator analysis identified that target gene networks of *Ppargc1a*, *Nfe2l2*, *Tgfb1*, *Ppara*, *Mapt*, and *Agt* decrease while *Txnrd1* and *Gsr* targets increase in E8G3 compared to E8G1 (Fig. 2E). We also created a network map of pathways, upstream regulators, and genes that were predicted to change between E8G1 and E8G3 (Fig. 2F). Genes that modulate the immune system like *Cd44, Cd38, Tnfsf11, Il5*, and *Il10ra* are predicted to be inhibited, while protein metabolism-related genes, *Arnt2, Rictor*, and *Lxr/Rxr* activation are predicted to be activated between E8G1 and E8G3. *Arnt* activity is predicted to be repressed in E8G3 compared to E8G1, leading to predicted decreases in triacylglycerol and acylglycerol in E8G3. In addition, *Nfe2l2*/NRF2-mediated oxidative stress responses that are upregulated in E8G1, are predicted to be downregulated in E8G3 perhaps due to reductions in oxidative stress in E8G3 (Fig. 2F).

While many of the differences between E8G1 and E8G3 likely play a role in the subsequent liver injury, there are clearly some protective and some injury promoting gene/pathways that decrease between E8G1 and E8G3, making it difficult to determine the changes that drive liver adaptation to binge ethanol. As genes that are up/downregulated 9h after the first binge are likely to play a role in subsequent binge ethanol-induced liver injury, we sought to determine which genes and pathways are similarly regulated in E8G1 and E8G3 to see whether continued activation of protective genes and pathways by binge ethanol play a role in liver protection. Therefore, we split the top differentially-regulated genes between P8w and E8G1 into four different groups – genes that are upregulated in E8G1 and either (1)

further increase (up-up) or (2) decrease in E8G3 (up-down); or genes that are downregulated in E8G1 and either (3) further decrease (down-down) or (4) increase (down-up) in E8G3 (Fig. 3A–B; Fig. S2C–D). Gene *Nlrp12* in the up-up group is a known hepatoprotective factor that may help to reduce liver injury in E8G3 while *Lcn2* promotes ethanol-induced liver injury; the roles of the genes in the down-down group have not been probed in ethanol-induced liver injury to our knowledge (Fig. 3A–B) (Zhang et al., 2020, Cai et al., 2016). Furthermore, we evaluated how the top upstream regulators and pathways in E8G1 vs. E8w compared to E8G3 vs. E8w. While there are some differences in pathway responses, including decreased NRF2-mediated oxidative stress response and increased LXR/RXR activation in E8G3, the activation status of most pathways and upstream regulators were similar between E8G1 and E8G3, indicating that these pathways may play a role in the reduced liver injury after E8G3 (Fig. 3C–D).

It is difficult to distinguish exactly how the identified genes, upstream regulators, and pathways contributes to liver injury in E8G3, as each could be protective, damaging, or have no effect on liver injury. However, the genes and pathways that are upregulated in E8G1 and continue to be upregulated in E8G3, despite reduced liver injury, are likely to play a role in adaptation to binge ethanol. Therefore, we decided to follow up on CYP2b10 as a potential protective factor in ethanol-induced liver injury as it was the highest upregulated gene in the up-up group and has no previous data on its role in ethanol-induced liver injury.

Hepatic *Cyp2b10* is upregulated after binge ethanol.

First, we decided to confirm the enhanced hepatic expression of Cyp2b10. As illustrated in Fig. 4A–C, qRT-PCR, western blot, and immunohistochemistry analyses revealed that *Cyp2b10*/CYP2B10 expression was slightly elevated after chronic ethanol (E8w) but highly increased after E8G1 or E8G3. In contrast, hepatic expression of related enzymes *Cyp2b9 and Cyp2b13* seem to be specifically responsive to chronic ethanol, as binge ethanol did not further increase their expression (Fig. 4A). In addition, chronic ethanol responsive CYP2E1 expression was equally upregulated in E8w, E8G1, and E8G3 groups compared to pair-fed P8W group, while hepatic expression of ADH1 showed consistent expression throughout the experiment (Fig. 4B).

Interestingly, while *Cyp2b10* is barely detected in normal mouse livers, *Cyp2b10* mRNA and CYP2B10 protein were detected at high levels in duodenal mucosa and jejunal mucosal where *Cyp2e1* and *Adh1* mRNA and proteins were detected at very low to undetected levels (Fig. S3). Immunohistochemistry analysis also confirmed that both duodenal and jejunal mucosal tissues expressed high levels of CYP2B10 proteins (Fig. S3), and the specificity of staining was confirmed in *Cyp2b10* KO mouse tissues (Data not shown). However, induction of *Cyp2b10* gene expression by ethanol did not occur in the duodenum indicating that the major effect of ethanol on *Cyp2b10* occurs in the liver (Fig. S4A).

To determine whether chronic ethanol feeding was required for *Cyp2b10* induction, we gave mice an acute gavage of ethanol (5g/kg) and checked liver mRNA expression of *Cyp2b10* at different time points. This data suggests that *Cyp2b10* is quickly induced by acute ethanol as early as 6h post gavage and returns to baseline by 24h (Fig. S4B). To investigate the mechanism of *Cyp2b10* induction, we attempted to use primary mouse hepatocytes. As seen

in a previous study (Koga et al., 2016), *Cyp2b10* induction with ethanol treatment *in vitro* is lackluster (Fig. S4C), suggesting that ethanol does not directly upregulate *Cyp2b10* in hepatocytes. However, it is also possible that we couldn't see the induction of *Cyp2b10* due to primary mouse hepatocytes quickly losing expression of metabolizing enzymes and some transcription factors after isolation.

CYP2B10 does not play a role in acute ethanol metabolism but may indirectly contribute to chronic plus binge ethanol clearance.

While CYP2b10 has known roles in xenobiotic and lipid metabolism, many members of the CYP2 family can metabolize ethanol as part of the microsomal ethanol oxidizing system. Therefore, we analyzed genes involved in ethanol oxidation from our microarray data, and Cyp2b10 is one of the few CYP2 family genes that is highly induced in E8G3 (Fig. 5A). To determine whether the induction of *Cyp2b10* after binge ethanol leads to changes in ethanol metabolism and liver injury, we generated *Cyp2b10* knockout (KO) mice and subjected them to the 8-week chronic plus one or three binges of ethanol model. We took blood samples 1h after the gavage of maltose/ethanol for each treatment group and sacrificed the mice 9h after the gavage to identify differences in liver injury. There were no differences in ethanol levels before gavage, but one hour after the first or third gavage, chronically ethanol-fed *Cyp2b10* KO mice exhibited significantly higher levels of ethanol compared to WT mice (Fig. 5B). To further identify the role of CYP2b10 in ethanol metabolism, we gave a single dose of ethanol to WT, *Cyp2b10* KO, or *Adh1* KO mice and measured serum ethanol concentrations at multiple time points. While *Adh1* KO mice had significantly higher levels of ethanol at all time points, there were no differences in ethanol concentrations between WT and *Cyp2b10* KO mice (Fig. 5C). To see if CYP2b10 can significantly contribute to microsomal ethanol metabolism, we extracted liver microsomes from WT or *Cyp2b10* KO mice treated with TCPOBOP, a *Cyp2b10* inducer, and measured ethanol oxidation to acetaldehyde *in vitro*. Control experiments confirmed TCPOBOP-mediated induction of CYP2B10 in microsomes and CYP2B10 inhibitors were working correctly (Fig. S5). Concentration-dependent ethanol metabolism did not differ in vehicle or TCPOBOP-treated mouse microsomes (Fig. 5D). In addition, *Cyp2b10* induction with TCPOBOP or treatment with a CYP2b10 inhibitor (PPP) did not alter ethanol oxidation to acetaldehyde in either WT or *Cyp2b10* KO mice (Fig. 5E).

CYP2b10 protects against ethanol-induced liver damage but is not responsible for liver adaptation to binge ethanol.

To determine whether CYP2b10 plays a role in liver injury, we analyzed liver injury in the mice described above. Livers of WT and *Cyp2b10* KO mice after E8G1 were stained with H&E, MPO, and Sirius Red, and our data revealed that *Cyp2b10* KO mice had higher levels of steatosis, neutrophil infiltration, and fibrosis compared with WT mice (Fig. 6A). Accordingly, *Cyp2b10* KO mice showed significantly higher ALT levels and a trend of higher AST levels than WT after E8G1 (Fig. 6B–C). In addition, western blot analyses showed that *Cyp2b10* KO mice exhibited increased 4-HNE adducts after E8G1, indicating higher levels of lipid peroxidation in Cyp2b10 KO mice (Fig. 6D). However, it should be noted that the toxicological adaptation to binge ethanol still occurs in *Cyp2b10* KO mice as 4-HNE adducts, ALT, and AST levels in E8G3 groups were similarly decreased in both WT and *Cyp2b10* KO mice compared to those in E8G1 groups (Fig. 6B–D). Finally, serum

triglycerides or cholesterol levels were measured, and our data revealed that there were no differences in these parameters between *Cyp2b10* KO and WT mice post E8G1 or E8G3 exposure (Fig. S6A–B).

The human homolog for *Cyp2b10*, *CYP2B6*, plays an important role in liver homeostasis in addition to its well-known role in drug metabolism, as low CYP2B6 activity in human liver microsomes is associated with obesity (Krogstad et al., 2020). We sought to determine the expression pattern of *CYP2B6* in alcohol-associated liver diseases (ALD) and pulled RNA-seq expression data from the livers of healthy controls or patients with alcoholic steatohepatitis (ASH), severe alcoholic hepatitis (sAH), explanted alcoholic hepatitis (ExAH), non-alcoholic fatty liver disease (NAFLD), hepatitis C virus infected (HCV), and HCV progressed to cirrhosis (HCV Cirr) (Argemi et al., 2019, Kim et al., 2021). Interestingly, *CYP2B6* levels were decreased even in ASH, one of the early forms of alcoholic liver damage, as well as AH and both forms of HCV (Fig. S6C). However, *CYP2B6* expression is not decreased in NAFLD livers, indicating that such decreases are related to alcoholic liver damage or more severe forms of liver disease.

Metabolomics reveal significant differences in the livers of *Cyp2b10* KO and WT mice after chronic plus binge alcohol.

To determine the underlying mechanisms by which CYP2b10 protects against ethanol-induced liver damage, we submitted liver tissue or serum from WT and *Cyp2b10* KO mice (n=5) in the E8G1 group to metabolomics analysis. The partial least squares discriminate analysis (PLS-DA) plots for positive ion mode in both the liver and serum samples showed that there were significant changes in metabolomic profiles between WT and *Cyp2b10* mice after chronic plus binge ethanol (Fig. 7A–B). Over 200 features, including ~65 identified metabolites, were significantly different in the livers of *Cyp2b10* KO mice, confirming that CYP2b10 plays an important role in liver homeostasis after chronic plus binge ethanol (Fig. 7C). On the other hand, only ~75 features reached significance in serum of *Cyp2b10* KO mice with only 28 metabolites identified, showing that the biggest impact of CYP2b10 is in the liver (Fig. 7D). Several liver metabolites related to the gamma-glutamyl cycle and glutathione disposition were changed, including increases in 5-oxoproline (pyroglutamic acid/pyrrolidonecarboxylic acid), cysteinylglycine, glutathione, and glutathione disulfide, and a decrease in L-glutamic acid in *Cyp2b10* KO mice. In addition, glucuronide metabolites ethyl glucuronide and thyroxine glucuronide were increased in *Cyp2b10* KO liver (Fig. 7E). Major changes in serum metabolites included several carnitine metabolites that mostly decreased in the *Cyp2b10* KO mice. In addition, kynurenine exhibits drastic decreases in the *Cyp2b10* KO mouse serum compared to WT mice (Fig. 7F).

Discussion

Recent increases in ethanol consumption and ethanol-related deaths worldwide underscore the need to develop better models of acute-on-chronic alcohol-related liver disease. While the NIAAA model using 10 days or 8 weeks of chronic ethanol plus an acute gavage of ethanol recapitulates some alcohol-related liver pathology (Bertola et al., 2013b, Xu et al., 2015), there is always a need for a model that better captures the clinical features of such

liver injury. Therefore, we sought to modify the NIAAA model to add two additional binges over two days to potentially better model liver injury. Surprisingly, mice given three gavages of ethanol exhibited less liver injury, steatosis, and fibrosis, than mice given a single gavage of ethanol after chronic feeding.

To better understand how three binges caused less injury than one binge in chronically ethanol-fed mice, we performed microarray analysis of liver tissues alongside previously published samples (Xu et al., 2015). While a limitation of our study is that we did not collect E8G2 samples to better identify stepwise changes in liver gene expression, we were able to identify several pathways that likely contribute to liver adaptation to binge ethanol through bioinformatic analysis, including acute phase response and complement cascades. Gavage of high doses of ethanol is known to activate the acute phase response in a toll-like receptor 4-dependent manner, most likely due to the corresponding intestinal barrier dysfunction and translocation of gut bacteria (Pruett and Pruett, 2006). In addition, innate immunity and the complement system have been implicated in many facets of ALD (Santiesteban-Lores et al., 2021). While some complement factors are protective and some harmful in the pathogenesis of ALD, it seems that the induction of this pathway in E8G3 may function to protect against bacterial translocation similar to acute phase response (Cohen et al., 2010, Roychowdhury et al., 2009, Duan et al., 2021). Another pathway that changed in our analysis was oxidative phosphorylation between E8G1 and E8G3. Ethanol is known to significantly change the mitochondria of hepatocytes, triggering the formation of megamitochondria and mitophagy as protective mechanisms, so structural and functional changes to mitochondria should be further investigated as a potential protective mechanism in the E8G3 mice (Palma et al., 2019, Williams et al., 2015). One limitation of the current study is that we did not look at changes in the intestines and adipose tissues after E8G3 to see whether changes in those organs also influence liver adaptation to binge ethanol. As these organs play an important role in controlling ALD pathogenesis, future studies should look at whether these organs also adapt to binge ethanol and influence liver injury after E8G1 and E8G3.

When we looked deeper at the microarray data, we noticed that *Cyp2b10*, an ethanol metabolism related gene, was highly upregulated in both E8G1 and E8G3 in contrast to other upregulated genes that returned towards baseline in E8G3. Previous studies have shown that hepatic expression of *Cyp2b* enzymes can be upregulated by chronic ethanol in several different models (Schoedel et al., 2001, Choi et al., 2018, Koga et al., 2016). We confirmed that hepatic *Cyp2b10* expression is mildly induced after E8w, but highly induced after E8G1 and E8G3. Although *Cyp2b10* is highly expressed in the intestine, which was not significantly upregulated after ethanol feeding, ethanol induction of *Cyp2b10* seems to be restricted to the liver. Acute ethanol administration also induced liver *Cyp2b10* expression, and we sought to identify mechanisms behind *Cyp2b10* induction. Although we did not examine the molecular mechanisms underlying ethanol-mediated induction of liver *Cyp2b10* expression, several potential mechanisms are likely involved. First, bioinformatic analysis predicted activation of CAR in E8G1 and E8G3 (data not shown). CAR is a known *Cyp2b10* inducer (Chen et al., 2011), which probably contributes to binge ethanol induction of hepatic *Cyp2b10*. Second, both pregnane X receptor and peroxisome proliferator-activated receptor β/δ have been implicated in the control of hepatic *Cyp2b10* expression post chronic or binge ethanol feeding, and these mechanisms are likely also involved *Cyp2b10* induction

by acute-on-chronic ethanol (Choi et al., 2017, Choi et al., 2018, Koga et al., 2016). Another known mechanism that may contribute to ethanol-induced Cyp2b10 induction is the NRF2-mediated oxidative stress response, which is linked to activation of CAR and is highly upregulated after E8G1 based on our bioinformatic data (Ashino et al., 2014, Rooney et al., 2019). The human/monkey homolog of *Cyp2b10*, *CYP2B6*, is induced by ethanol self-administration in several brain regions of monkeys and studies in human brains strongly suggest that *CYP2B6* is elevated in certain brain regions of people with alcohol use disorder (AUD) (Ferguson et al., 2013, Miksys et al., 2003). While these studies focus on CYP2B6 in the brain, they provide evidence that ethanol may be able to induce CYP2B6 in humans.

Previous studies suggest that CYP2B6 has the ability to metabolize ethanol, but these studies did not further characterize how CYP2B6 regulates ethanol metabolism (Vuppugalla et al., 2007, Busby et al., 1999, Hamitouche et al., 2006). Our data showed that *Cyp2b10* KO mice exhibit higher ethanol concentrations than WT mice after E8G1 and E8G3. However, *Cyp2b10* KO and WT mice had comparable levels of blood ethanol concentrations after acute ethanol administration, and *in vitro* studies of microsomal ethanol metabolism revealed that CYP2B10 did not directly participate in ethanol metabolism. Taken together, our data suggest that CYP2B10 indirectly promotes ethanol metabolism during chronic ethanol consumption. Further studies are required to clarify the mechanisms by which CYP2B10 regulates chronic ethanol metabolism. In addition, we also found that CYP2B10 is protective against ethanol-induced liver injury as *Cyp2b10* KO mice exhibited increased liver injury (ALT), steatosis, fibrosis, and lipid peroxidation after E8G1 compared to WT mice. However, CYP2B10 is not responsible for the liver adaptation to binge ethanol as injury still decreased in *Cyp2b10* KO mice from E8G1 to E8G3. While the increased ethanol concentrations in *Cyp2b10* KO mice may contribute to the increased liver injury, CYP2B enzymes are known to play other physiological roles. Studies in *Cyp2b*-knockdown and null mice have shown that CYP2B enzymes have sexually dimorphic effects on lipid homeostasis, with male *Cyp2b*-knockdown/null mice gaining more weight on HFD (Damiri and Baldwin, 2018, Heintz et al., 2019, Heintz et al., 2020, Heintz et al., 2022). In addition, studies using conditional P450 oxioreductase (POR) mice and *Cyp2b*-knockdown mice provided evidence that CYP2B enzymes are likely involved in unsaturated fatty acid metabolism (Damiri and Baldwin, 2018, Finn et al., 2009). These potential endogenous roles of CYP2B enzymes led us to conduct metabolomic analyses for WT and *Cyp2b10* KO mice after E8G1 to determine the mechanism behind CYP2B10 protection against ethanol-induced liver injury.

Liver and serum metabolomics were clearly different between WT and *Cyp2b10* KO mice after E8G1, with major differences seen in liver nucleotides, amino acids, glutathione, fatty acids and lipid precursors, and sugars. The increase in ethyl glucuronide, a marker of ethanol use, in *Cyp2b10* KO mice correlates well with our data that ethanol levels are elevated after E8G1 as compared to WT mice. One of the highest elevated metabolites (7-fold) in the livers of *Cyp2b10* KO mice was 5-oxoproline (pyroglutamic acid/pyrrolidonecarboxylic acid), which is a participant in the gamma-glutamyl cycle that leads to glutathione synthesis. Elevated levels of 5-oxoproline are associated with high anion gap metabolic acidosis, a serious condition that can be induced by acetaminophen (Tailor et al., 2005, Alhourani et al., 2018, Fenves et al., 2006). The enzyme 5-oxoprolinase (*Oplah*) converts 5-oxoproline

to L-glutamate, and since liver 5-oxoproline is increased and L-glutamate is decreased, 5-oxoprolinase may be dysfunctional in *Cyp2b10* KO mice. However, this does not seem to disrupt glutathione synthesis as glutathione and glutathione disulfide are both upregulated in *Cyp2b10* KO mice. Glucose-6-phosphate (G6P) is another metabolite that is highly upregulated in the livers of *Cyp2b10* KO mice, and accumulation of G6P has been shown in liver samples from patients with alcohol-associated hepatitis when compared to control samples due to upregulation of hexokinase domain containing 1 (Massey et al., 2021). Future studies should identify how CYP2B10 affects energy balance in ethanol-treated livers.

To determine how these studies may translate to humans, we analyzed results from a previously published RNA-seq dataset that identified gene expression in livers of patients exhibiting different types of liver injury (Kim et al., 2021, Argemi et al., 2019). The human homolog of *Cyp2b10*, *CYP2B6*, was downregulated in early alcohol-associated steatohepatitis and severe alcohol-associated hepatitis (AH) but unchanged in non-alcoholic fatty liver disease. These alcohol-related liver disease samples were from patients without recent binge drinking, which may be the reason CYP2B6 was not highly upregulated because upregulation of hepatic *Cyp2b10* expression was transient after acute ethanol gavage. These decreases in *CYP2B6* expression in AH are associated with decreases in microRNA-148a, which stabilizes CYP2B6 mRNA and leads to increased transcription, and this mechanism may explain the discrepancies between mice and humans (Luo et al., 2021). Regardless, if CYP2B6 is a protective factor for ALD in humans like CYP2B10 in mice, the decreased CYP2B6 expression in ALD patients may be detrimental. CYP2B6 is also a highly polymorphic enzyme, with several genetic variants having allele frequencies of >30% which significantly reduce enzyme expression or activity (Zanger et al., 2007). The association of CYP2B6 polymorphisms with progression of ALD should be further investigated to help clarify the role of CYP2B6 in ALD. In summary, these studies demonstrated a novel model (E8G3) to study liver (and perhaps other organ) adaptation to binge ethanol, identified Cyp2b10 as a protective factor for acute-on-chronic ethanol-induced liver injury, and provide evidence to further study the role of Cyp2b10 homolog CYP2B6 in human ALD.

Supplementary Material

Refer to Web version on PubMed Central for supplementary material.

Acknowledgments

This work was supported by the intramural program of NIAAA, NIH (BG) and grant R21 AA028521AA028521 (HW). No conflicts of interest exist for any of the authors.

References:

Alhourani HM, Kumar A, George LK, Sarwar T, Wall BM (2018) Recurrent Pyroglutamic Acidosis Related to Therapeutic Acetaminophen. The American Journal of the Medical Sciences 355:387–389. [PubMed: 29661353]

Anvret A, Ran C, Westerlund M, Gellhaar S, Lindqvist E, Pernold K, Lundstromer K, Duester G, Felder MR, Galter D, Belin AC (2012) Adh1 and Adh1/4 knockout mice as possible rodent models for presymptomatic Parkinson's disease. Behav Brain Res 227:252–257. [PubMed: 22079585]

Argemi J, Latasa MU, Atkinson SR, Blokhin IO, Massey V, Gue JP, Cabezas J, Lozano JJ, Van Booven D, Bell A, Cao S, Vernetti LA, Arab JP, Ventura-Cots M, Edmunds LR, Fondevilla C, Stärkel P, Dubuquoy L, Louvet A, Odena G, Gomez JL, Aragon T, Altamirano J, Caballeria J, Jurczak MJ, Taylor DL, Berasain C, Wahlestedt C, Monga SP, Morgan MY, Sancho-Bru P, Mathurin P, Furuya S, Lackner C, Rusyn I, Shah VH, Thursz MR, Mann J, Avila MA, Bataller R (2019) Defective HNF4alpha-dependent gene expression as a driver of hepatocellular failure in alcoholic hepatitis. Nature Communications 10:3126.

Ashino T, Ohkubo-Morita H, Yamamoto M, Yoshida T, Numazawa S (2014) Possible involvement of nuclear factor erythroid 2-related factor 2 in the gene expression of Cyp2b10 and Cyp2a5. Redox Biol 2:284–288. [PubMed: 24494203]

Attal N, Sullivan MT, Girardi CA, Thompson KJ, McKillop IH (2021) Fatty acid binding protein-4 promotes alcohol-dependent hepatosteatosis and hepatocellular carcinoma progression. Transl Oncol 14:100975. [PubMed: 33290990]

Bellentani S, Saccoccio G, Costa G, Tiribelli C, Manenti F, Sodde M, Croce' LS, Sasso F, Pozzato G, Cristianini G, Brandi, the Dionysos Study Group G (1997) Drinking habits as cofactors of risk for alcohol induced liver damage. Gut 41:845. [PubMed: 9462221]

Bertola A, Mathews S, Ki SH, Wang H, Gao B (2013a) Mouse model of chronic and binge ethanol feeding (the NIAAA model). Nat Protoc 8:627–637. [PubMed: 23449255]

Bertola A, Park O, Gao B (2013b) Chronic plus binge ethanol feeding synergistically induces neutrophil infiltration and liver injury in mice: a critical role for E-selectin. Hepatology 58:1814–1823. [PubMed: 23532958]

Busby WF, Ackermann JM, Crespi CL (1999) Effect of Methanol, Ethanol, Dimethyl Sulfoxide, and Acetonitrile on In Vitro Activities of cDNA-Expressed Human Cytochromes P-450. Drug Metabolism and Disposition 27:246. [PubMed: 9929510]

Cai Y, Jogasuria A, Yin H, Xu MJ, Hu X, Wang J, Kim C, Wu J, Lee K, Gao B, You M (2016) The Detrimental Role Played by Lipocalin-2 in Alcoholic Fatty Liver in Mice. Am J Pathol 186:2417–2428. [PubMed: 27427417]

Cederbaum AI (2010) Role of CYP2E1 in ethanol-induced oxidant stress, fatty liver and hepatotoxicity. Dig Dis 28:802–811. [PubMed: 21525766]

Cederbaum AI (2012) Alcohol metabolism. Clin Liver Dis 16:667–685. [PubMed: 23101976]

Chen X, Meng Z, Wang X, Zeng S, Huang W (2011) The nuclear receptor CAR modulates alcohol-induced liver injury. Lab Invest 91:1136–1145. [PubMed: 21519326]

Choi S, Gyamfi AA, Neequaye P, Addo S, Gonzalez FJ, Gyamfi MA (2018) Role of the Pregnane X Receptor in Binge Ethanol-Induced Steatosis and Hepatotoxicity. Journal of Pharmacology and Experimental Therapeutics 365:165. [PubMed: 29431616]

Choi S, Neequaye P, French SW, Gonzalez FJ, Gyamfi MA (2017) Pregnane X receptor promotes ethanol-induced hepatosteatosis in mice. J Biol Chem.

Chun J, Kent UM, Moss RM, Sayre LM, Hollenberg PF (2000) Mechanism-Based Inactivation of Cytochromes P450 2B1 and P450 2B6 by 2-Phenyl-2-(1-piperidinyl)propane. Drug Metabolism and Disposition 28:905. [PubMed: 10901699]

Cohen JI, Roychowdhury S, McMullen MR, Stavitsky AB, Nagy LE (2010) Complement and Alcoholic Liver Disease: Role of C1q in the Pathogenesis of Ethanol-Induced Liver Injury in Mice. Gastroenterology 139:664–674.e661. [PubMed: 20416309]

Damiri B, Baldwin WS (2018) Cyp2b-Knockdown Mice Poorly Metabolize Corn Oil and Are Age-Dependent Obese. Lipids 53:871–884. [PubMed: 30421529]

Deltour L, Foglio MH, Duester G (1999) Metabolic Deficiencies in Alcohol Dehydrogenase Adh1,Adh3, and Adh4 Null Mutant Mice: OVERLAPPING ROLES OF Adh1 AND Adh4 IN ETHANOL CLEARANCE AND METABOLISM OF RETINOL TO RETINOIC ACID *. Journal of Biological Chemistry 274:16796–16801. [PubMed: 10358022]

Duan Y, Chu H, Brandl K, Jiang L, Zeng S, Meshgin N, Papachristoforou E, Argemi J, Mendes BG, Wang Y, Su H, Sun W, Llorente C, Hendrikx T, Liu X, Hosseini M, Kisseleva T, Brenner DA,

Bataller R, Ramachandran P, Karin M, Fu W, Schnabl B (2021) CRIg on liver macrophages clears pathobionts and protects against alcoholic liver disease. Nature Communications 12:7172.

Fenves AZ, Kirkpatrick HM, Patel VV, Sweetman L, Emmett M (2006) Increased Anion Gap Metabolic Acidosis as a Result of 5-Oxoproline (Pyroglutamic Acid): A Role for Acetaminophen. Clinical Journal of the American Society of Nephrology 1:441. [PubMed: 17699243]

Ferguson CS, Miksys S, Palmour RM, Tyndale RF (2013) Ethanol self-administration and nicotine treatment induce brain levels of CYP2B6 and CYP2E1 in African green monkeys. Neuropharmacology 72:74–81. [PubMed: 23639433]

Finn RD, Henderson CJ, Scott CL, Wolf CR (2009) Unsaturated fatty acid regulation of cytochrome P450 expression via a CAR-dependent pathway. Biochem J 417:43–54. [PubMed: 18778245]

Gao B, Bataller R (2011) Alcoholic Liver Disease: Pathogenesis and New Therapeutic Targets. Gastroenterology 141:1572–1585. [PubMed: 21920463]

Ghosh Dastidar S, Warner JB, Warner DR, McClain CJ, Kirpich IA (2018) Rodent Models of Alcoholic Liver Disease: Role of Binge Ethanol Administration. Biomolecules 8.

Gonzalez FJ, Ueno T, Umeno M, Song BJ, Veech RL, Gelboin HV (1991) Microsomal ethanol oxidizing system: transcriptional and posttranscriptional regulation of cytochrome P450, CYP2E1. Alcohol Alcohol Suppl 1:97–101. [PubMed: 1845601]

Griswold MG, Fullman N, Hawley C, Arian N, Zimsen SRM, Tymeson HD, Venkateswaran V, Tapp AD, Forouzanfar MH, Salama JS, Abate KH, Abate D, Abay SM, Abbafati C, Abdulkader RS, Abebe Z, Aboyans V, Abrar MM, Acharya P, Adetokunboh OO, Adhikari TB, Adsuar JC, Afarideh M, Agardh EE, Agarwal G, Aghayan SA, Agrawal S, Ahmed MB, Akibu M, Akinyemiju T, Akseer N, Asfoor DHA, Al-Aly Z, Alahdab F, Alam K, Albujeer A, Alene KA, Ali R, Ali SD, Alijanzadeh M, Aljunid SM, Alkerwi Aa, Allebeck P, Alvis-Guzman N, Amare AT, Aminde LN, Ammar W, Amoako YA, Amul GGH, Andrei CL, Angus C, Ansha MG, Antonio CAT, Aremu O, Ärnlöv J, Artaman A, Aryal KK, Assadi R, Ausloos M, Avila-Burgos L, Avokpaho EF, Awasthi A, Ayele HT, Ayer R, Ayuk TB, Azzopardi PS, Badali H, Badawi A, Banach M, Barker-Collo SL, Barrero LH, Basaleem H, Baye E, Bazargan-Hejazi S, Bedi N, Béjot Y, Belachew AB, Belay SA, Bennett DA, Bensenor IM, Bernabe E, Bernstein RS, Beyene AS, Beyranvand T, Bhaumik S, Bhutta ZA, Biadgo B, Bijani A, Bililign N, Birlik SM, Birungi C, Bizuneh H, Bjerregaard P, Bjørge T, Borges G, Bosetti C, Boufous S, Bragazzi NL, Brenner H, Butt ZA, Cahuana-Hurtado L, Calabria B, Campos-Nonato IR, Campuzano JC, Carreras G, Carrero JJ, Carvalho F, Castañeda-Orjuela CA, Castillo Rivas J, Catalá-López F, Chang J-C, Charlson FJ, Chattopadhyay A, Chaturvedi P, Chowdhury R, Christopher DJ, Chung S-C, Ciobanu LG, Claro RM, Conti S, Cousin E, Criqui MH, Dachew BA, Dargan PI, Daryani A, Das Neves J, Davletov K, De Castro F, De Courten B, De Neve J-W, Degenhardt L, Demoz GT, Des Jarlais DC, Dey S, Dhaliwal RS, Dharmaratne SD, Dhimal M, Doku DT, Doyle KE, Dubey M, Dubljanin E, Duncan BB, Ebrahimi H, Edessa D, El Sayed Zaki M, Ermakov SP, Erskine HE, Esteghamati A, Faramarzi M, Farioli A, Faro A, Farvid MS, Farzadfar F, Feigin VL, Felisbino-Mendes MS, Fernandes E, Ferrari AJ, Ferri CP, Fijabi DO, Filip I, Finger JD, Fischer F, Flaxman AD, Franklin RC, Futran ND, Gallus S, Ganji M, Gankpe FG, Gebregergs GB, Gebrehiwot TT, Geleijnse JM, Ghadimi R, Ghandour LA, Ghimire M, Gill PS, Ginawi IA, Giref AZZ, Gona PN, Gopalani SV, Gotay CC, Goulart AC, Greaves F, Grosso G, Guo Y, Gupta R, Gupta R, Gupta V, Gutiérrez RA, Gvs M, Hafezi-Nejad N, Hagos TB, Hailu GB, Hamadeh RR, Hamidi S, Hankey GJ, Harb HL, Harikrishnan S, Haro JM, Hassen HY, Havmoeller R, Hay SI, Heibati B, Henok A, Heredia-Pi I, Hernández-Llanes NF, Herteliu C, Hibstu DTT, Hoogar P, Horita N, Hosgood HD, Hosseini M, Hostiuc M, Hu G, Huang H, Husseini A, Idrisov B, Ileanu BV, Ilesanmi OS, Irvani SSN, Islam SMS, Jackson MD, Jakovljevic M, Jalu MT, Jayatilleke AU, Jha RP, Jonas JB, Jozwiak JJ, Kabir Z, Kadel R, Kahsay A, Kapil U, Kasaeian A, Kassa TDD, Katikireddi SV, Kawakami N, Kebede S, Kefale AT, Keiyoro PN, Kengne AP, Khader Y, Khafaie MA, Khalil IA, Khan MN, Khang Y-H, Khater MM, Khubchandani J, Kim C-I, Kim D, Kim YJ, Kimokoti RW, Kisa A, Kivimäki M, Kochhar S, Kosen S, Koul PA, Koyanagi A, Krishan K, Kuate Defo B, Kucuk Bicer B, Kulkarni VS, Kumar P, Lafranconi A, Lakshmana Balaji A, Lalloo R, Lallukka T, Lam H, Lami FH, Lan Q, Lang JJ, Lansky S, Larsson AO, Latifi A, Leasher JL, Lee PH, Leigh J, Leinsalu M, Leung J, Levi M, Li Y, Lim L-L, Linn S, Liu S, Lobato-Cordero A, Lopez AD, Lorkowski S, Lotufo PA, Macarayan ERK, Machado IE, Madotto F, Magdy Abd El Razek H, Magdy Abd El Razek M, Majdan M, Majdzadeh R, Majeed A, Malekzadeh R, Malta DC, Mapoma CC, Martinez-Raga

J, Maulik PK, Mazidi M, McKee M, Mehta V, Meier T, Mekonen T, Meles KG, Melese A, Memiah PTN, Mendoza W, Mengistu DT, Mensah GA, Meretoja TJ, Mezgebe HB, Miazgowski T, Miller TR, Mini G, Mirica A, Mirrakhimov EM, Moazen B, Mohammad KA, Mohammadifard N, Mohammed S, Monasta L, Moraga P, Morawska L, Mousavi SM, Mukhopadhyay S, Musa KI, Naheed A, Naik G, Najafi F, Nangia V, Nansseu JR, Nayak MSDP, Nejjari C, Neupane S, Neupane SP, Ngunjiri JW, Nguyen CT, Nguyen LH, Nguyen TH, Ningrum DNA, Nirayo YL, Noubiap JJ, Ofori-Asenso R, Ogbo FA, Oh I-H, Oladimeji O, Olagunju AT, Olivares PR, Olusanya BO, Olusanya JO, Oommen AM, Oren E, Orpana HM, Ortega-Altamirano DDV, Ortiz JR, Ota E, Owolabi MO, Oyekale AS, P A M, Pana A, Park E-K, Parry CDH, Parsian H, Patle A, Patton GC, Paudel D, Petzold M, Phillips MR, Pillay JD, Postma MJ, Pourmalek F, Prabhakaran D, Qorbani M, Radfar A, Rafay A, Rafiei A, Rahim F, Rahimi-Movaghar A, Rahman M, Rahman MA, Rai RK, Rajsic S, Raju SB, Ram U, Rana SM, Ranabhat CL, Rawaf DL, Rawaf S, Reiner RC, Reis C, Renzaho AMN, Rezai MS, Roever L, Ronfani L, Room R, Roshandel G, Rostami A, Roth GA, Roy A, Sabde YD, Saddik B, Safiri S, Sahebkar A, Salama JS, Saleem Z, Salomon JA, Salvi SS, Sanabria J, Sanchez-Niño MD, Santomauro DF, Santos IS, Santric Milicevic MMM, Sarker AR, Sarmiento-Suárez R, Sarrafzadegan N, Sartorius B, Satpathy M, Sawhney M, Saxena S, Saylan M, Schaub MP, Schmidt MI, Schneider IJC, Schöttker B, Schutte AE, Schwendicke F, Sepanlou SG, Shaikh MA, Sharif M, She J, Sheikh A, Shen J, Shiferaw MS, Shigematsu M, Shiri R, Shishani K, Shiue I, Shukla SR, Sigfusdottir ID, Silva DAS, Silva NTD, Silveira DGA, Sinha DN, Sitas F, Soares Filho AM, Soofi M, Sorensen RJD, Soriano JB, Sreeramareddy CT, Steckling N, Stein DJ, Sufiyan MaB, Sur PJ, Sykes BL, Tabarés-Seisdedos R, Tabuchi T, Tavakkoli M, Tehrani-Banihashemi A, Tekle MG, Thapa S, Thomas N, Topor-Madry R, Topouzis F, Tran BX, Troeger CE, Truelsen TC, Tsilimparis N, Tyrovolas S, Ukwaja KN, Ullah I, Uthman OA, Valdez PR, Van Boven JFM, Vasankari TJ, Venketasubramanian N, Violante FS, Vladimirov SK, Vlassov V, Vollset SE, Vos T, Wagnew FWS, Waheed Y, Wang Y-P, Weiderpass E, Weldegebreal F, Weldegwergs KG, Werdecker A, Westerman R, Whiteford HA, Widecka J, Wijeratne T, Wyper GMA, Xu G, Yamada T, Yano Y, Ye P, Yimer EM, Yip P, Yirsaw BD, Yisma E, Yonemoto N, Yoon S-J, Yotebieng M, Younis MZ, Zachariah G, Zaidi Z, Zamani M, Zhang X, Zodpey S, Mokdad AH, Naghavi M, Murray CJL, Gakidou E (2018) Alcohol use and burden for 195 countries and territories, 1990–2016: a systematic analysis for the Global Burden of Disease Study 2016. The Lancet 392:1015–1035.

Hamitouche S, Poupon J, Dreano Y, Amet Y, Lucas D (2006) Ethanol oxidation into acetaldehyde by 16 recombinant human cytochrome P450 isoforms: Role of CYP2C isoforms in human liver microsomes. Toxicology Letters 167:221–230. [PubMed: 17084997]

Heintz MM, Kumar R, Maner-Smith KM, Ortlund EA, Baldwin WS (2022) Age- and Diet-Dependent Changes in Hepatic Lipidomic Profiles of Phospholipids in Male Mice: Age Acceleration in Cyp2b-Null Mice. Journal of Lipids 2022:7122738. [PubMed: 35391786]

Heintz MM, Kumar R, Rutledge MM, Baldwin WS (2019) Cyp2b-null male mice are susceptible to diet-induced obesity and perturbations in lipid homeostasis. The Journal of Nutritional Biochemistry 70:125–137. [PubMed: 31202118]

Heintz MM, McRee R, Kumar R, Baldwin WS (2020) Gender differences in diet-induced steatotic disease in Cyp2b-null mice. PLOS ONE 15:e0229896. [PubMed: 32155178]

Hu M, Yin H, Mitra MS, Liang X, Ajmo JM, Nadra K, Chrast R, Finck BN, You M (2013) Hepatic-specific lipin-1 deficiency exacerbates experimental alcohol-induced steatohepatitis in mice. Hepatology 58:1953–1963. [PubMed: 23787969]

Ki SH, Park O, Zheng M, Morales-Ibanez O, Kolls JK, Bataller R, Gao B (2010) Interleukin-22 treatment ameliorates alcoholic liver injury in a murine model of chronic-binge ethanol feeding: role of signal transducer and activator of transcription 3. Hepatology 52:1291–1300. [PubMed: 20842630]

Kim A, Wu X, Allende DS, Nagy LE (2021) Gene Deconvolution Reveals Aberrant Liver Regeneration and Immune Cell Infiltration in Alcohol-Associated Hepatitis. Hepatology 74:987–1002. [PubMed: 33619773]

Koga T, Yao P-L, Goudarzi M, Murray IA, Balandaram G, Gonzalez FJ, Perdew GH, Fornace AJ, Peters JM (2016) Regulation of Cytochrome P450 2B10 (CYP2B10) Expression in Liver by Peroxisome Proliferator-activated Receptor-β/δ Modulation of SP1 Promoter Occupancy. Journal of Biological Chemistry 291:25255–25263. [PubMed: 27765815]

Krogstad V, Peric A, Robertsen I, Kringen MK, Wegler C, Angeles PC, Hjelmesæth J, Karlsson C, Andersson S, Artursson P, Åsberg A, Andersson TB, Christensen H (2020) A Comparative Analysis of Cytochrome P450 Activities in Paired Liver and Small Intestinal Samples from Patients with Obesity. Drug Metab Dispos 48:8–17. [PubMed: 31685482]

Lubet RA, Mayer RT, Cameron JW, Nims RW, Burke MD, Wolff T, Guengerich FP (1985) Dealkylation of pentoxyresorufin: a rapid and sensitive assay for measuring induction of cytochrome(s) P-450 by phenobarbital and other xenobiotics in the rat. Arch Biochem Biophys 238:43–48. [PubMed: 3985627]

Lucey MR, Mathurin P, Morgan TR (2009) Alcoholic Hepatitis. New England Journal of Medicine 360:2758–2769. [PubMed: 19553649]

Luo J, Xie M, Hou Y, Ma W, Jin Y, Chen J, Li C, Zhao K, Chen N, Xu L, Ji Y, Zhang Q, Zheng Y, Yu D (2021) A novel epigenetic mechanism unravels hsa-miR-148a-3p-mediated CYP2B6 downregulation in alcoholic hepatitis disease. Biochemical Pharmacology 188:114582. [PubMed: 33895159]

Massey V, Parrish A, Argemi J, Moreno M, Mello A, García-Rocha M, Altamirano J, Odena G, Dubuquoy L, Louvet A, Martinez C, Adrover A, Affò S, Morales-Ibanez O, Sancho-Bru P, Millán C, Alvarado-Tapias E, Morales-Arraez D, Caballería J, Mann J, Cao S, Sun Z, Shah V, Cameron A, Mathurin P, Snider N, Villanueva C, Morgan TR, Guinovart J, Vadigepalli R, Bataller R (2021) Integrated Multiomics Reveals Glucose Use Reprogramming and Identifies a Novel Hexokinase in Alcoholic Hepatitis. Gastroenterology 160:1725–1740.e1722. [PubMed: 33309778]

Miksys S, Lerman C, Shields PG, Mash DC, Tyndale RF (2003) Smoking, alcoholism and genetic polymorphisms alter CYP2B6 levels in human brain. Neuropharmacology 45:122–132. [PubMed: 12814665]

Palma E, Ma X, Riva A, Iansante V, Dhawan A, Wang S, Ni HM, Sesaki H, Williams R, Ding WX, Chokshi S (2019) Dynamin-1-Like Protein Inhibition Drives Megamitochondria Formation as an Adaptive Response in Alcohol-Induced Hepatotoxicity. Am J Pathol 189:580–589. [PubMed: 30553835]

Pang Z, Chong J, Zhou G, de Lima Morais DA, Chang L, Barrette M, Gauthier C, Jacques PE, Li S, Xia J (2021) MetaboAnalyst 5.0: narrowing the gap between raw spectra and functional insights. Nucleic Acids Res 49:W388–W396. [PubMed: 34019663]

Pruett BS, Pruett SB (2006) An explanation for the paradoxical induction and suppression of an acute phase response by ethanol. Alcohol 39:105–110. [PubMed: 17134663]

Ren T, Mackowiak B, Lin Y, Gao Y, Niu J, Gao B (2020) Hepatic injury and inflammation alter ethanol metabolism and drinking behavior. Food Chem Toxicol 136:111070. [PubMed: 31870920]

Rooney JP, Oshida K, Kumar R, Baldwin WS, Corton JC (2019) Chemical Activation of the Constitutive Androstane Receptor Leads to Activation of Oxidant-Induced Nrf2. Toxicol Sci 167:172–189. [PubMed: 30203046]

Roy N, Dasgupta D, Mukhopadhyay I, Chatterjee A, Das K, Bhowmik P, Das S, Basu P, Santra AK, Datta S, Dhali GK, Chowdhury A, Banerjee S (2016) Genetic Association and Gene-Gene Interaction Reveal Genetic Variations in ADH1B, GSTM1 and MnSOD Independently Confer Risk to Alcoholic Liver Diseases in India. PLoS One 11:e0149843. [PubMed: 26937962]

Roychowdhury S, McMullen MR, Pritchard MT, Hise AG, van Rooijen N, Medof ME, Stavitsky AB, Nagy LE (2009) An early complement-dependent and TLR-4–independent phase in the pathogenesis of ethanol-induced liver injury in mice. Hepatology 49:1326–1334. [PubMed: 19133650]

Sahi J, Hamilton G, Sinz M, Barros S, Huang SM, Lesko LJ, LeCluyse EL (2000) Effect of troglitazone on cytochrome P450 enzymes in primary cultures of human and rat hepatocytes. Xenobiotica 30:273–284. [PubMed: 10752642]

Santiesteban-Lores LE, Carneiro MC, Isaac L, Bavia L (2021) Complement System in Alcohol-Associated Liver Disease. Immunology Letters 236:37–50. [PubMed: 34111475]

Schoedel KA, Sellers EM, Tyndale RF (2001) Induction of CYP2B1/2 and nicotine metabolism by ethanol in rat liver but not rat brain22Abbreviations: CYP, cytochrome P450; C8 xanthate, potassium octylxanthate; NCO, nicotine C-oxidation; NDMA, N-nitrosodimethylamine; NMA, N-nitroso-N-methylaniline; NNK, 4-(methylnitrosamino)-1-(3-pyridyl)-1-butanone; and SSC, saline-sodium citrate buffer. Biochemical Pharmacology 62:1025–1036. [PubMed: 11597571]

Tailor P, Raman T, Garganta CL, Njalsson R, Carlsson K, Ristoff E, Carey HB (2005) Recurrent High Anion Gap Metabolic Acidosis Secondary to 5-Oxoproline (Pyroglutamic Acid). American Journal of Kidney Diseases 46:e4–e10. [PubMed: 15983950]

Vuppugalla R, Chang S-Y, Zhang H, Marathe PH, Rodrigues DA (2007) Effect of Commonly Used Organic Solvents on the Kinetics of Cytochrome P450 2B6- and 2C8-Dependent Activity in Human Liver Microsomes. Drug Metabolism and Disposition 35:1990. [PubMed: 17709370]

Walsky RL, Obach RS (2007) A comparison of 2-phenyl-2-(1-piperidinyl)propane (ppp), 1,1',1"-phosphinothioylidynetrisaziridine (thioTEPA), clopidogrel, and ticlopidine as selective inactivators of human cytochrome P450 2B6. Drug Metab Dispos 35:2053–2059. [PubMed: 17682072]

Williams JA, Ni HM, Ding Y, Ding WX (2015) Parkin regulates mitophagy and mitochondrial function to protect against alcohol-induced liver injury and steatosis in mice. Am J Physiol Gastrointest Liver Physiol 309:G324–340. [PubMed: 26159696]

Wishart DS, Guo A, Oler E, Wang F, Anjum A, Peters H, Dizon R, Sayeeda Z, Tian S, Lee BL, Berjanskii M, Mah R, Yamamoto M, Jovel J, Torres-Calzada C, Hiebert-Giesbrecht M, Lui VW, Varshavi D, Varshavi D, Allen D, Arndt D, Khetarpal N, Sivakumaran A, Harford K, Sanford S, Yee K, Cao X, Budinski Z, Liigand J, Zhang L, Zheng J, Mandal R, Karu N, Dambrova M, Schioth HB, Greiner R, Gautam V (2022) HMDB 5.0: the Human Metabolome Database for 2022. Nucleic Acids Res 50:D622–D631. [PubMed: 34986597]

Xu M-J, Cai Y, Wang H, Altamirano J, Chang B, Bertola A, Odena G, Lu J, Tanaka N, Matsusue K, Matsubara T, Mukhopadhyay P, Kimura S, Pacher P, Gonzalez FJ, Bataller R, Gao B (2015) Fat-Specific Protein 27/CIDEC Promotes Development of Alcoholic Steatohepatitis in Mice and Humans. Gastroenterology 149:1030–1041.e1036. [PubMed: 26099526]

Zakhari S, Li T-K (2007) Determinants of alcohol use and abuse: Impact of quantity and frequency patterns on liver disease. Hepatology 46:2032–2039. [PubMed: 18046720]

Zanger UM, Klein K, Saussele T, Blievernicht J, Hofmann MH, Schwab M (2007) Polymorphic CYP2B6: molecular mechanisms and emerging clinical significance. Pharmacogenomics 8:743–759. [PubMed: 17638512]

Zhang YF, Bu FT, Yin NN, Wang A, You HM, Wang L, Jia WQ, Huang C, Li J (2020) NLRP12 negatively regulates EtOH-induced liver macrophage activation via NF-kappaB pathway and mediates hepatocyte apoptosis in alcoholic liver injury. Int Immunopharmacol 88:106968. [PubMed: 33182058]

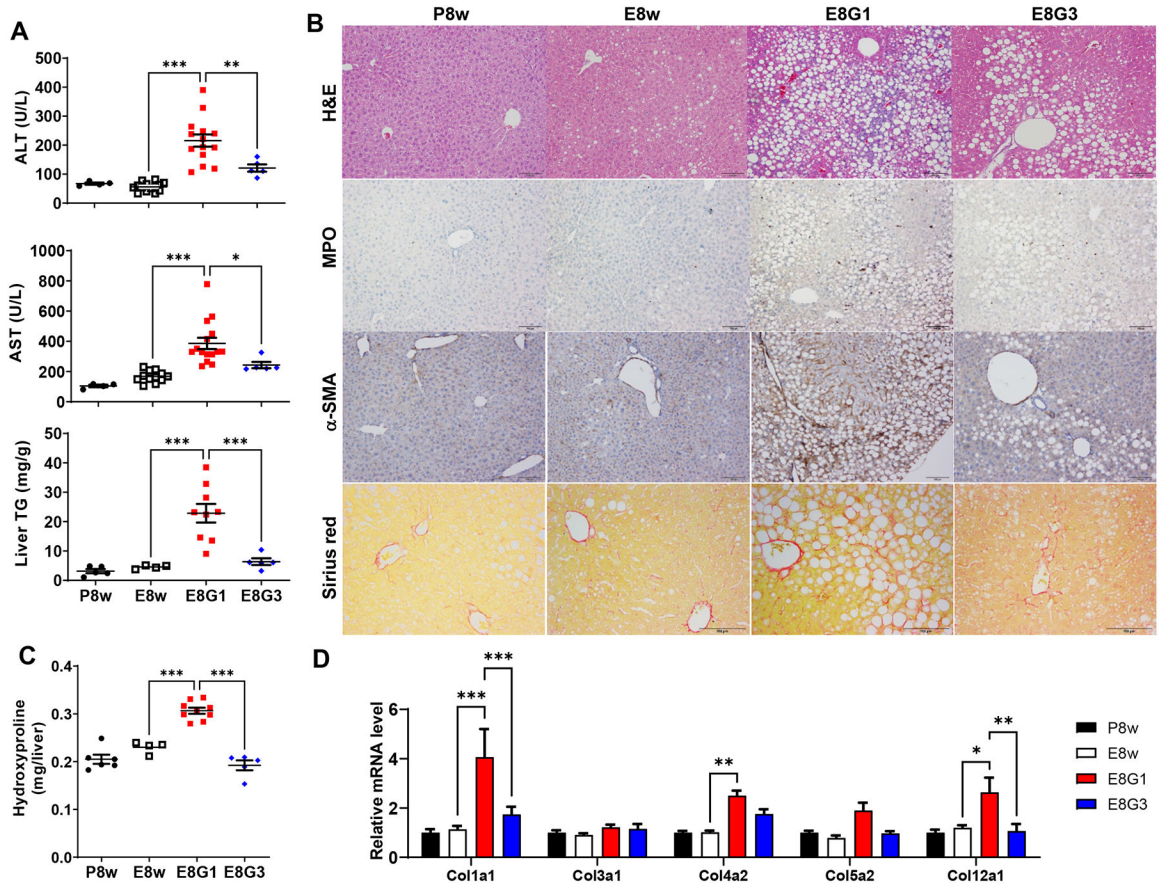

Figure 1: Three binges cause less liver damage and fibrosis than one binge in chronically ethanol-fed mice.

Eight to ten week-old male C57BL6N mice were fed a liquid diet containing 5% ethanol for 8 weeks and then received one maltose gavage (E8w), one ethanol binge (E8G1) or three ethanol binges (every 24 hours) (E8G3), or pair-fed (P8w); the mice were euthanized at 9 hours after the final binge. (A) Serum ALT, AST, and liver TG levels. (B) Representative images of H&E staining, anti-MPO and anti-α-SMA staining, and sirus red staining of livers. (C) Liver collagen content was assayed by determination of hydroxyproline content. (D) RT-qPCR analyses of gene expression in the liver tissue. Values represent the mean ± SEM (n=5–15 mice per group). **P*<0.05, ***P*<0.01, ****P*<0.001 as indicated.

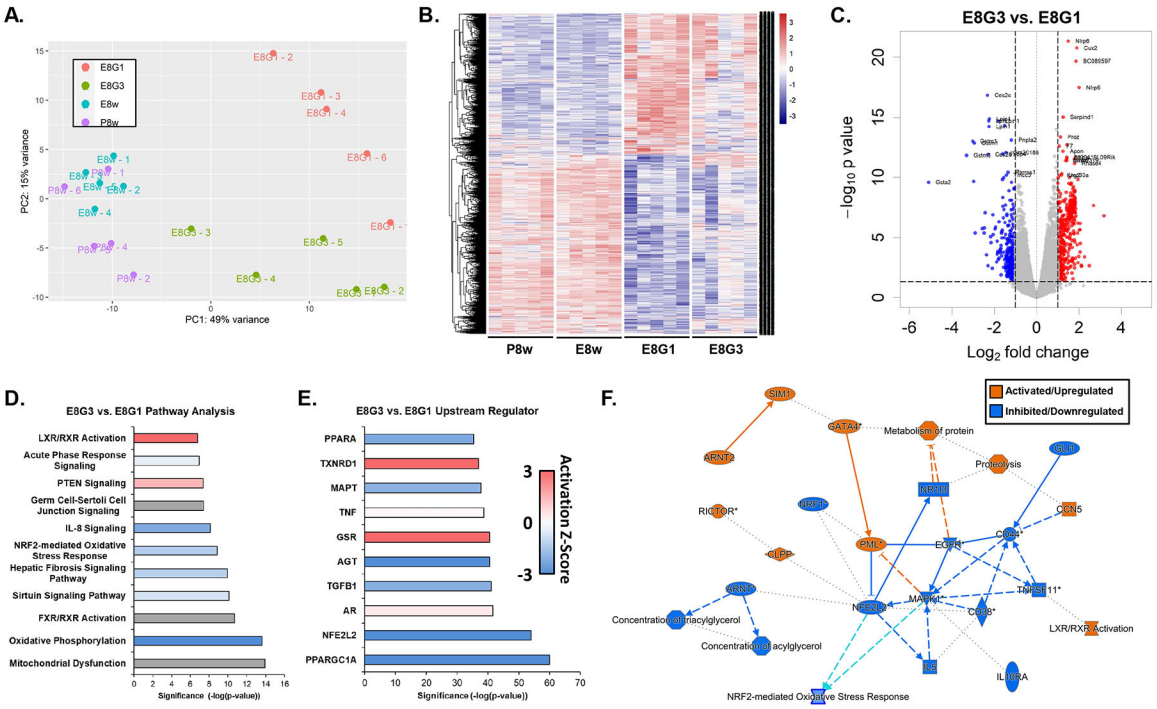

Figure 2: Microarray comparison of gene expression and pathway analyses of E8G3 vs. E8G1.

(A) Principal component analysis (PCA) plot of microarray data. (B) Heatmap of genes significantly changed between E8G1 compared to E8w. (C) Volcano plot of genes significantly changed between E8G3 and E8G1. (D) IPA analyses identified significant pathways and upstream regulators changed in E8G3 vs. E8G1. The color of each bar indicates the predicted activation of each pathway/upstream regulator (Grey indicates not enough data to predict activation state). (E) IPA network plot of significantly altered regulators and pathways between E8G3 and E8G1.

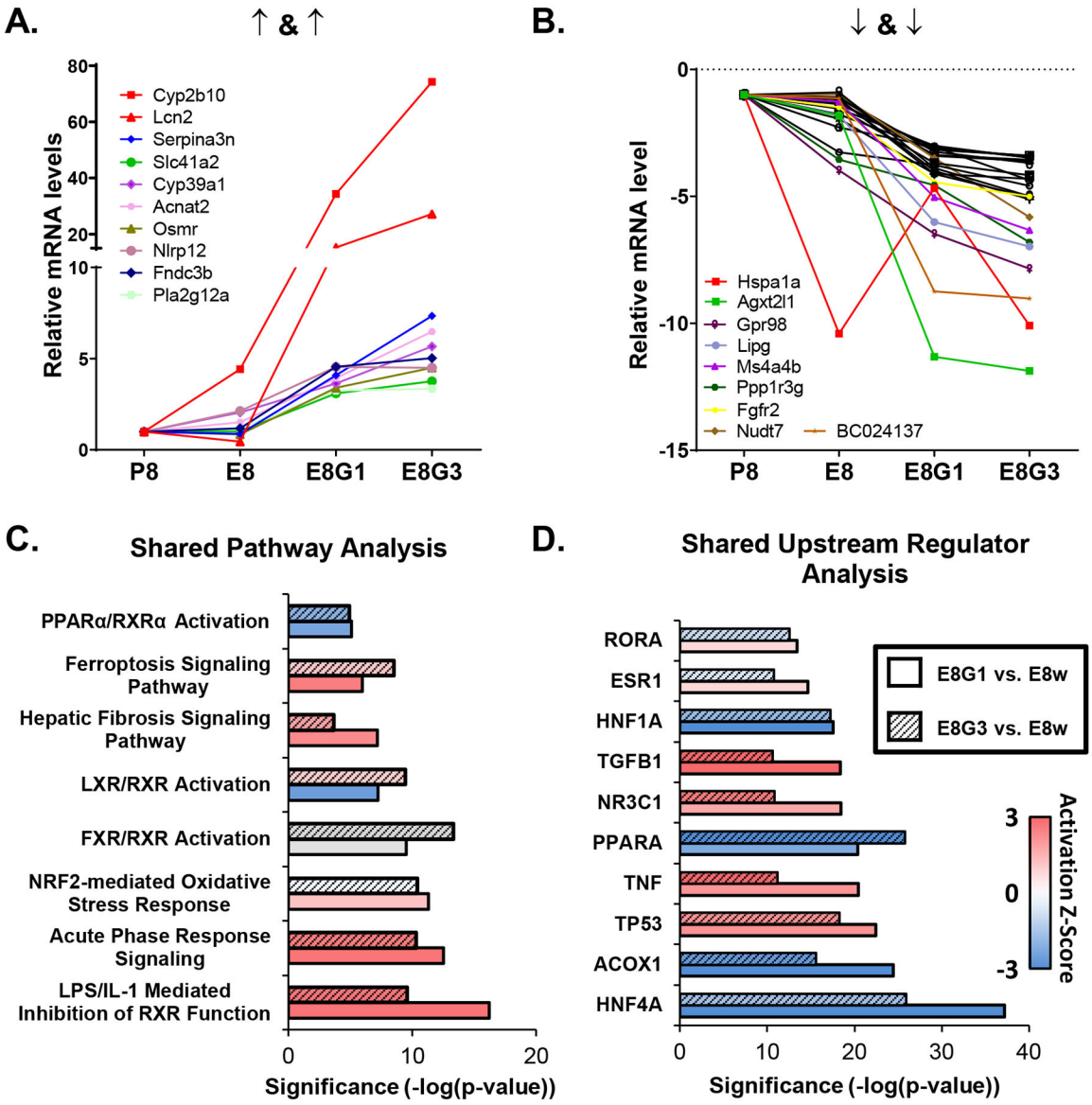

Figure 3: Similar gene and pathway regulation in E8G1 and E8G3.

(A-B) The average fold change of top up and downregulated genes in E8G1 compared to P8w that are further upregulated (A; up-up) or further downregulated (B; down-down) in E8G3. (C-D) IPA analyses identified top significant pathways and upstream regulators changed in E8G1 and E8G3 vs. E8w and the color of each bar indicates the predicted activation of each pathway/upstream regulator (Grey indicates not enough data to predict activation state).

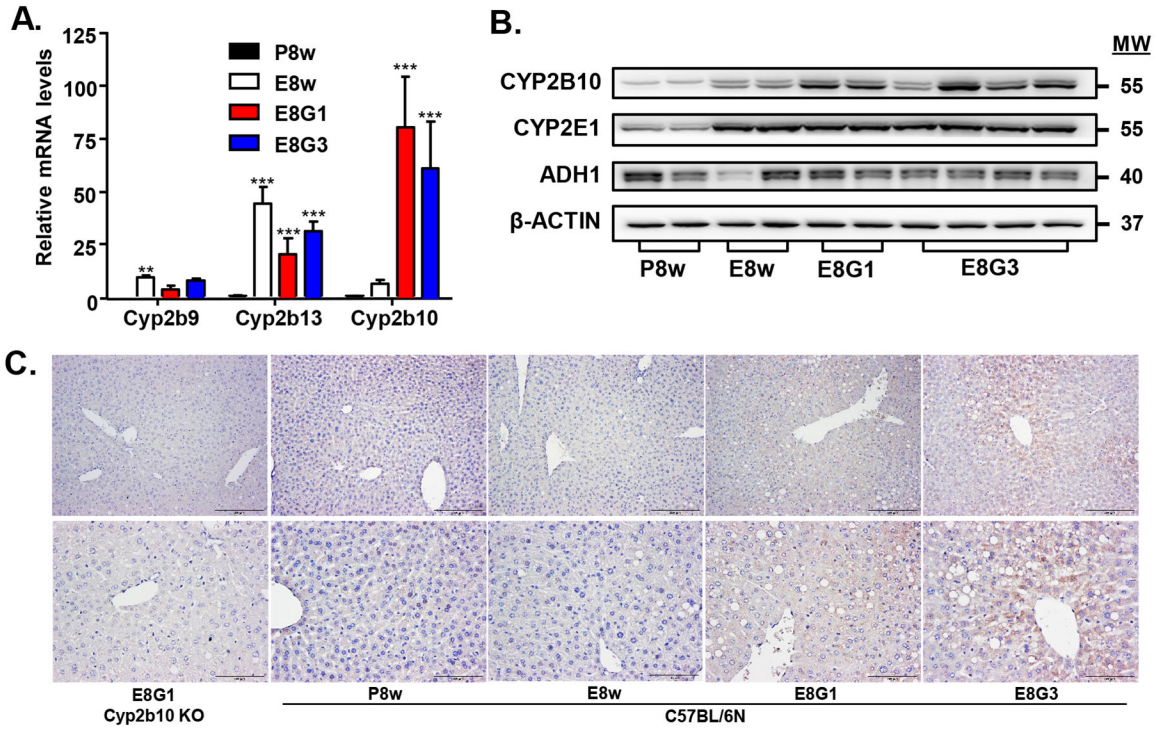

Figure 4: Hepatic *Cyp2b10* is specifically induced by binge ethanol.

(A) RT-qPCR analyses of *Cyp2b9*, *Cyp2b10* and *Cyp2b13* gene expression in the livers of pair, E8w, E8G1, E8G3 fed mice (n=5). (B) The protein levels of CYP2B10, CYP2E1, and ADH1 in the livers of P8w, E8w, E8G1, E8G3 fed mice. (C) Representative images of immunohistochemical (IHC) staining of CYP2B10 in the liver of P8w, E8w, E8G1, and E8G3. Values represent the mean ± SEM (n=3–5 mice per group). **P*<0.05, ***P*<0.01, ****P*<0.001 compared to WT as indicated.

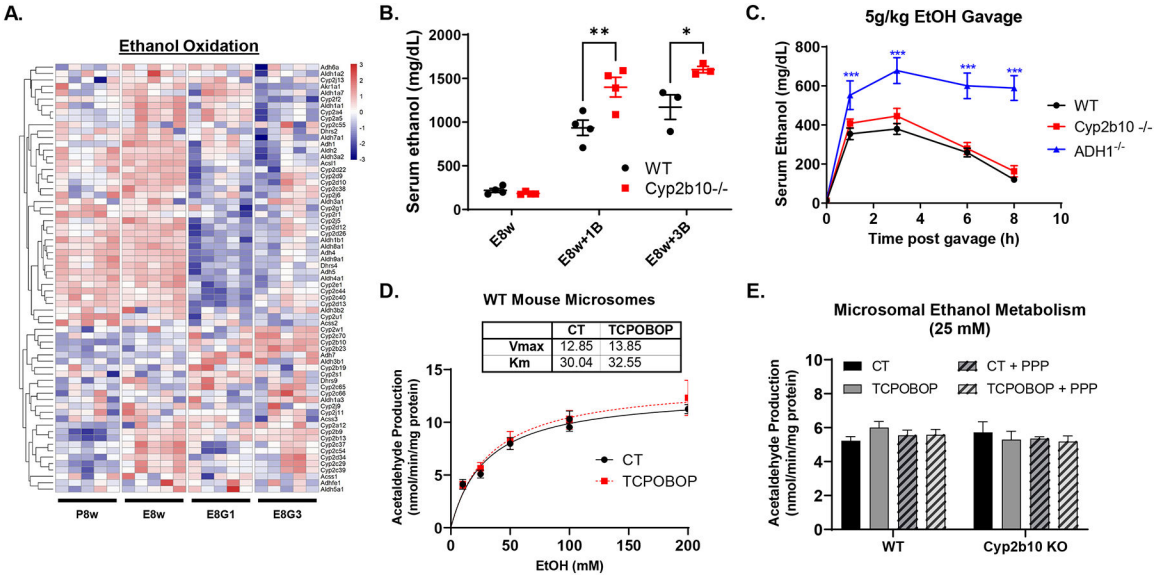

Figure 5. Ethanol metabolism is altered in *Cyp2b10* KO mice, but CYP2B10 does not directly participate in ethanol metabolism.

(A) Heatmap of ethanol oxidation genes identified in IPA. (B) Mice were fed with ethanol diet for 8 weeks. Blood ethanol levels were measured before gavage, and 1 h after either E8G1 or E8G3 (5 g/kg). (C) WT, *Cyp2b10* KO, and *Adh1* knockout mice received acute ethanol binge (5 g/kg). Blood ethanol levels were measured at 0 (before gavage) and 1, 3, 6, 8 h post-gavage. (D-E) Microsomes were isolated from the livers of WT or *Cyp2b10* KO mice either treated with TCPOBOP or vehicle for 24h. Microsomes were challenged with different concentrations of ethanol (C) or 25 mM ethanol with or without PPP, a Cyp2b inhibitor and acetaldehyde production was measured after 30 min (D). * $P<0.05$, ** $P<0.01$, *** $P<0.05$ as indicated

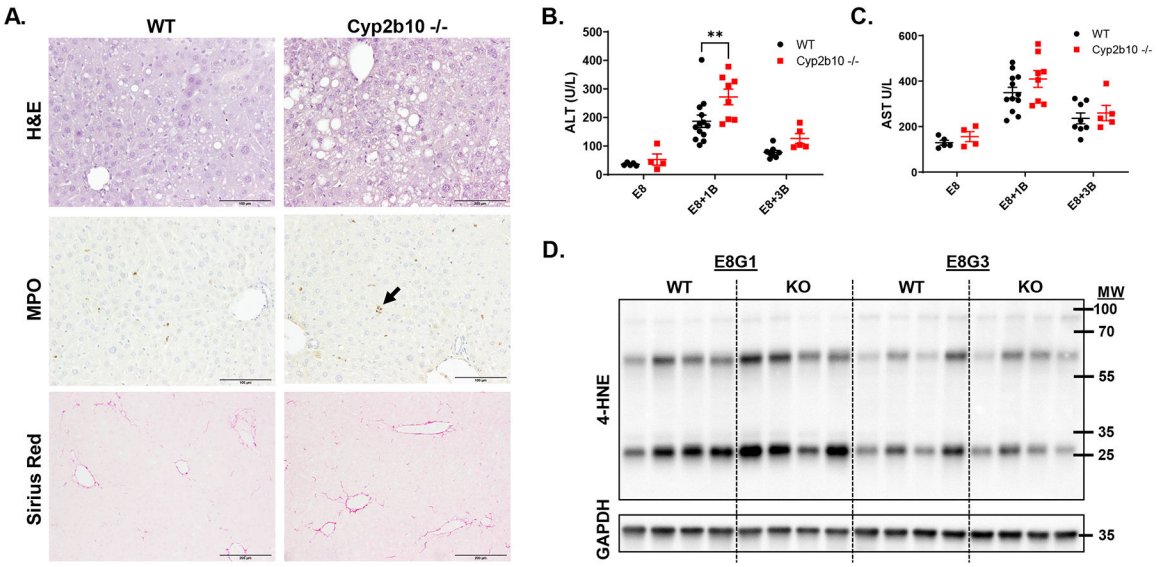

Figure 6. Genetic deletion of the *Cy2b10* gene exacerbates chronic-plus-binge ethanol-induced liver injury in mice.

WT and *Cyp2b10* KO mice received E8w, E8G1, or E8G3. (A) Representative images from E8G1 WT and *Cyp2b10* KO mice with H&E staining, anti-MPO, and sirus red staining of liver sections. (B) ALT and (C) AST were measured in male mice (n=4~7). (D) Western blot of 4-HNE in livers of WT and *Cyp2b10* mice after E8G1 and E8G3. * P<0.05 as indicated.

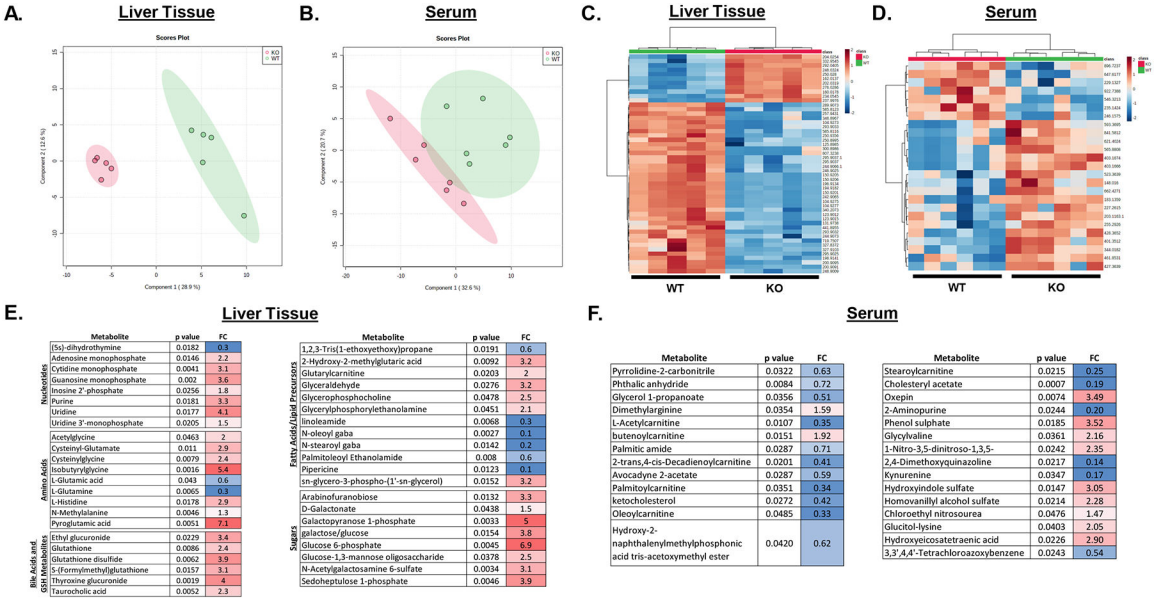

Figure 7. Metabolomics analysis of WT and Cyp2b10 KO mice.

WT and Cyp2b10 KO mice were subjected to E8G1 before analyzing serum and liver samples (n=6) by untargeted metabolomic analysis. Partial least squares discriminate analysis (PLS-DA) plots for positive ion mode (A,D) and metabolite heatmaps (B,E) were generated for both the liver (A,B) and serum (D,E) samples. Metabolites that were significantly changed are listed for liver (C) and serum (F) samples, with red highlights signifying increases in Cyp2b10 KO vs. WT and blue highlights indicating decreases in Cyp2b10 KO vs. WT.